sustainability

MDPI

Article

Micro- and Nano-Bubbles Enhanced the Treatment of an Urban Black-Odor River

Qinqin Xu, Zheng Zhou and Xiaoli Chai *

State Key Laboratory of Pollution Control and Resource Reuse, College of Environmental Science and Engineering, Tongji University, Shanghai 200092, China; qinqinxu@tongji.edu.cn (Q.X.); 1830551@tongji.edu.cn (Z.Z.)

* Correspondence: xlchai@tongji.edu.cn

Abstract: Black-odor water is prevalent in southeastern coastal regions of China, compromising both the aquatic ecosystem and urban aesthetics. Micro- and nano-bubbles (MNBs) aeration, identified as an innovative approach, offers potential improvements in water ecological function. This study introduces and implements an MNBs technique to rehabilitate an urban black-odor river. Results indicate that MNBs aeration achieved a significantly higher increment rate of dissolved oxygen (89.4%) and higher removal efficiencies of biological oxygen demand (54.4%), chemical oxygen demand (39.0%), ammonia nitrogen (63.2%), total phosphorus (28.0%) and dimethyl trisulfide (100%) in the water compared to conventional blast aeration. Concurrently, a 25.0% increase in the ratio of iron/aluminum-bonded phosphorus (Fe/Al-P) to total sediment phosphorus effectively curtailed endogenous phosphorus release. Additionally, MNBs aeration markedly reduced plankton biomass, suggesting direct removal by MNBs. This enhanced performance is attributable to the improved oxygen mass transfer coefficient and oxygenation capacity, fostering more efficient pollutants. Furthermore, MNBs significantly encouraged the growth of aerobic microorganisms (e.g., *Actinobacteria*, *Firmicutes* and *Myxococcota*) in the sediment, bolstering the water's self-purification ability. Consequently, this study validates MNBs as a highly promising solution for treating black odorous water bodies.

Keywords: micro- and nano-bubbles; black-odor river; plankton; microbial community

check for updates

Citation: Xu, Q.; Zhou, Z.; Chai, X. Micro- and Nano-Bubbles Enhanced the Treatment of an Urban Black-Odor River. *Sustainability* **2023**, *15*, 16695. https://doi.org/10.3390/su152416695

Academic Editor: Giovanni De Feo

Received: 24 October 2023
Revised: 24 November 2023
Accepted: 29 November 2023
Published: 9 December 2023

Copyright: © 2023 by the authors. Licensee MDPI, Basel, Switzerland. This article is an open access article distributed under the terms and conditions of the Creative Commons Attribution (CC BY) license (https://creativecommons.org/licenses/by/4.0/).

1. Introduction

The rapid urbanization and industrialization have significantly compromised water environments [1]. A considerable influx of pollutants, such as those from domestic sewage and industrial effluents, results in elevated levels of chemical oxygen demand (COD), suspended solids, nitrogen, phosphorus and other contaminants in aquatic systems [2–4]. This accumulation of pollutants depletes oxygen in water bodies, promoting the production of blackening materials and odorous gases. Such changes not only impair the water's ecosystem structure and self-purification ability but also cause sensory discomfort to residents and mar the urban landscape [5,6]. A 2016 report indicated that approximately 73% of 295 Chinese cities at the prefecture level and above were afflicted with black-odor water bodies [7]. In response, the Chinese government launched the "Action Plan for Water Pollution Prevention and Control" in 2015, aiming to eliminate over 90% of black-odor rivers by 2020 and virtually all such rivers by 2030 [8]. Consequently, the issue of black-odor water has emerged as a critical environmental challenge, necessitating prompt and effective restoration measures.

Over the years, aeration technology has increasingly been utilized to address black-odor water issues, owing to its notable enhancement of water self-purification [9,10]. Among various methods, micro- and nano-bubbles (MNBs), characterized by their longevity, minimal buoyancy and high gas solubility, have emerged as particularly effective in wastewater treatment [11–13]. MNBs offer two primary advantages: firstly, their larger surface

area facilitates more efficient O_2 mass transfer, and the elevated vapor pressure of O_2 enhances the solubility of dissolved oxygen (DO) [14]. Secondly, the collapse of MNBs generates a range of reactive oxygen species, such as superoxide anion radicals ($O_2\cdot^-$) and singlet oxygen ($^1O_2$)), which possess strong oxidative properties conducive to pollutant degradation [15,16]. Comparative studies have shown that MNBs aeration can deliver oxygen transfer efficiency more than tenfold higher and reduce oxygen decline rates by over 50% compared to macro-bubble aeration [4]. Furthermore, MNBs distinctly improve the removal of total organic carbon (TOC), COD, ammonia nitrogen (NH_3-N), Total Nitrogen (TN), total phosphorus (TP), odorous compounds (e.g., dimethyl trisulfide (DMTS) and 2-methylisotethanol (2-MIB)) and black substances (e.g., fulvic acid) and obviously expedite the microbial activities of nitrification and aerobic ammonia oxidation in polluted water bodies [4,9,10,17]. For instance, MNBs aeration achieved approximately 15% higher TOC and NH_3-N removal efficiencies compared to traditional aeration in treating livestock wastewater [10]. DMTS content in black-odor water was reduced by 99% within two hours under MNBs treatment, compared to a 67% reduction over one day with blast aeration [18]. In small water bodies, nearly all microorganisms in the MNBs treatment system were aerobic microbes, whereas no significant differences were noted between the percentage of aerobic microorganisms, contrasting the balanced presence of aerobic and anaerobic microorganisms in traditional macro-bubble aeration systems [17]. Therefore, MNBs demonstrate a superior capability in pollutant removal relative to conventional aeration techniques.

In China, approximately 60% of the black-odor rivers are concentrated in the more developed southeastern coastal areas. Among these, Tangmenbang, situated in the Yangtze River Delta economic circle, exemplifies a typical polluted urban black-odor river, characterized by its gray-black color with a pungent odor. To address this issue, an MNBs technology, founded on the principle of gas–liquid high-speed hydraulic spinning, was developed specifically for river remediation. In the current study, the objectives were as follows: (1) to investigate the physicochemical properties of the urban black-odor river; (2) to evaluate the effects of MNBs aeration on water and sediment quality; (3) to examine the responses of plankton composition and the microbial community to MNBs aeration.

2. Materials and Methods

2.1. Study Area

Tangmenbang, an urban river characterized by its distinct black odor, is situated in Changzhou, Jiangsu Province, China (refer to Figure 1). This river spans 1.5 km in length and 20 meters in width. It features two sluice gates that regulate water flow, often resulting in stagnant conditions. Along its course, 31 effluent discharge points have been identified, releasing various types of waste including domestic and industrial sewage. Notably, seven of these points remain actively operational (as detailed in Supplementary Materials Figure S1). Additionally, the riverbanks are marred by the accumulation of household refuse. Direct discharges into the river from sources such as livestock breeding facilities, septic tanks, and untreated initial rainwater runoff further contribute to its complex pollution profile.

2.2. Experiment Settings and Sample Collection

Three experimental sites along the river, designated as T1, T2 and T3, were selected for study (see Figure 1). Site T1 served as control, Site T2 employed blast aerators, and Site T3 utilized MNBs generators. The blast aerators operated using a high-pressure eddy fan, providing air at 0.029 MPa and 80 m^3/h, in conjunction with aeration discs for bubble production. MNBs aeration, based on gas–liquid high-speed hydraulic spinning, involved a gas–liquid mixing pump and a bubble generator, detailed in Supplementary Materials Section S2. The MNBs equipment operated at an outlet pressure of 0.55 MPa and an air intake of 3.5 m^3/h. The resultant bubble size predominantly ranged from 20 to 30 μm in diameter (refer to Figure 2a) [18]. A comparative analysis indicated the reoxygenation

capacity of MNBs was significantly superior to blast aeration, as evidenced by the Mann–Whitney U test ($p < 0.001$) (see Figure 2b).

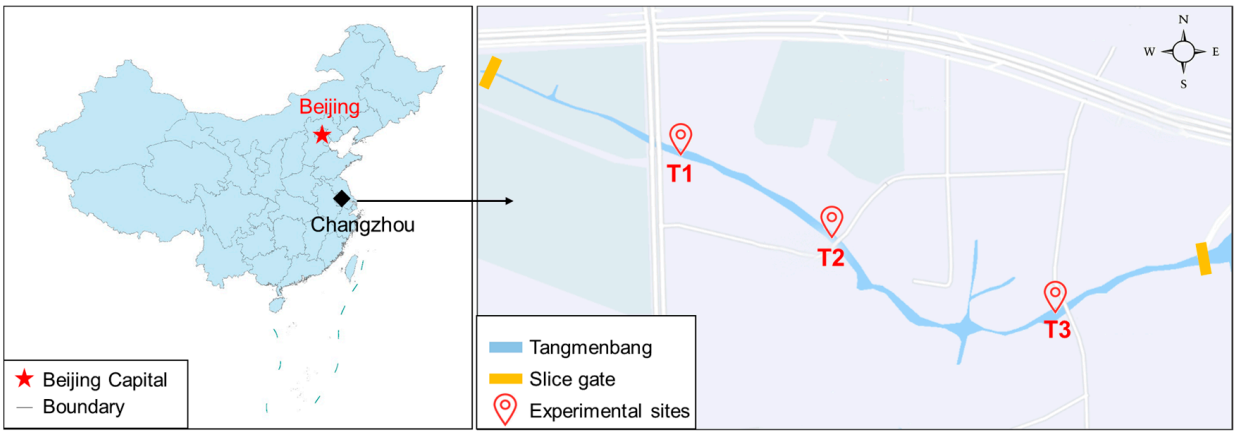

Figure 1. Distribution of the experimental sites in the Tangmenbang River.

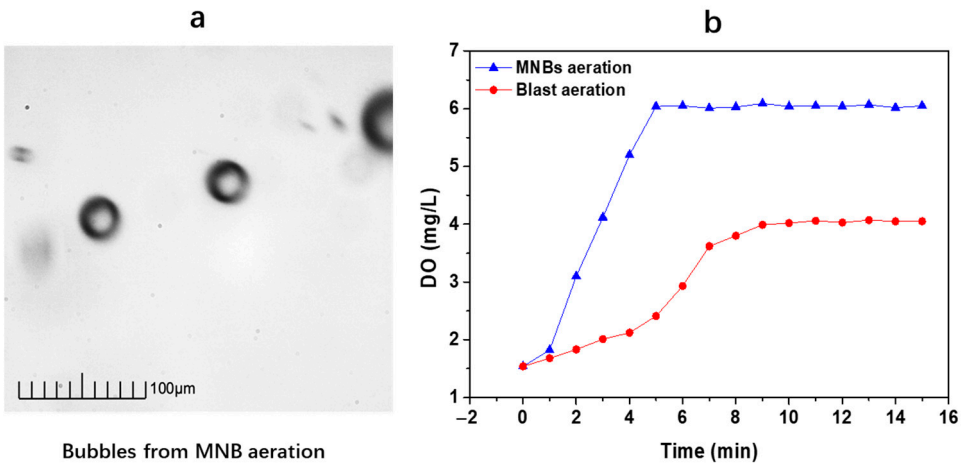

Figure 2. (**a**) Bubbles from MNBs aeration. (**b**) Reoxygenation curves for blast aeration and MNBs aeration.

2.3. Analytical Methods

2.3.1. Physicochemical Parameters of Water and Sediment

Dissolved Oxygen (DO), pH and Oxidation-Reduction Potential (OPR) were quantified in situ in triplicate, using a multi-parameter water quality analyzer (HQ30d, Hach, Loveland, CO, USA). Water transparency and the concentrations of inorganic anions (e.g., SO_4^{2-} and NO_x^-) were assessed using a Secchi disk and ion chromatography, respectively [2,19]. COD and biological oxygen demand (BOD) were evaluated following standard methods [7]. Total organic carbon (TOC) for water and sediment samples was determined with a TOC-L analyzer (Shimadzu Corp., Kyoto, Japan). Total Nitrogen (TN) in water was quantified using an alkaline potassium persulfate digestion UV spectrophotometric method, while sediment was measured through the semi-micro Kjeldahl method [19,20]. Ammonia nitrogen (NH_3-N) in water samples was analyzed via Nessler's reagent spectrophotometry; for sediments, NH_3-N was extracted using potassium chloride solution spectrophotometry [19]. Nitrate nitrogen (NO_x-N) in sediment samples was determined through phenol disulfonic acid colorimetry [21]. Total phosphorus (TP) in water samples was measured by ammonium molybdate spectrophotometric method, and phosphorus fractions in sediments were examined with the SMT sequential method [7,22]. The concentrations of metals, such as iron (Fe) and manganese (Mn), were quantified using Inductively Coupled Plasma Mass Spectrometry (ICP-MS, Thermo ICapQ, Thermo-Fisher Scientifc Inc., Dreieich, Germany) [23]. Dimethyl trisulfide (DMTS) was analyzed via Gas Chromatography–Mass

Spectrometry (GC-MS, 7890A-5975C, Agilent Technology Co., Ltd., Santa Clara, CA, USA) following Solid Phase Microextraction (50/30 μm PDMS/CAR/DVB (2 cm), Supelco, Bellefonte, PA, USA) [24]. Analytical accuracy was verified through the concurrent analysis of calibration curves, repeated testing, and method blanks.

2.3.2. Plankton Analysis

Ten-liter water samples were sequentially filtered on-site using a No. 25 plankton net (mesh 0.064 mm) and a No. 13 plankton net (mesh 0.112 mm) to isolate plankton, followed by the addition of Lugol's solution for preservation. Plankton enumeration was performed using a calibrated microscope, adopting a methodology outlined in a prior study [25]. A 0.1 mL aliquot of each sample was placed in a Sedgewick–Rafter counting chamber and examined under a microscope at either 8 × 40-fold or 10 × 40 magnification. Each sample underwent duplicate counts. In cases where the variance between the two counts exceeded 15%, a third count was conducted for accuracy.

2.3.3. DNA Extraction, Q-PCR Amplification and High-Throughput Sequencing

DNA from sediment samples was extracted utilizing the PowerSoil DNA Isolation kit (MoBio Laboratories, San Diego, CA, USA) in accordance with the provided manufacturer's protocol. The concentration and purity of the extracted DNA were quantified using a NanoDrop 2000 (Thermo Fisher Scientific, Waltham, MA, USA). Polymerase chain reaction (PCR) amplification was conducted with the ABI-7500 PCR system (Applied Biosystems, Waltham, MA, USA). High-throughput sequencing was carried out on the Illumine NovaSeq 6000 platform, following established protocols, and executed by Majorbio Bio-pharm Technology Co., Ltd. (Shanghai, China). The V4 region of 16 S rRNA gene was amplified using primers 515FmodF (5′-GTGYCAGCMGCCGCGGTAA-3′) and 806RmodR (5′-GGACTACNVGGGTWTCTAAT-3′) [26]. Operational taxonomic units (OTUs) were identified at a 97% threshold using Uparse software (Uparse v.7.0.1001) [1].

2.4. Statistical Analysis

The Shannon–Wiener diversity index (S-W) was computed to analyze the diversity characteristics of the plankton community [27]. To assess significant differences between paired or unpaired samples, statistical analyses including the Mann–Whitney U test, Kruskal–Wallis test and Fisher's exact test were utilized. Significant differences were all declared at $p < 0.05$.

3. Results and Discussion

3.1. Physicochemical Characteristics of the Urban Black-Odor River

The physicochemical properties of water in Tangmenbang River are summarized in Table 1. As per China's "Working guidelines for the treatment of urban black-odor water" [28], black-odor intensity is categorized as mild (transparency = 10–25 cm, DO = 0.2–2.0 mg/L, ORP = −200–50 mV, NH_3-N = 8.0–15.0 mg/L) and severe (transparency < 10 cm, DO < 0.2 mg/L, ORP < −200 mV, NH_3-N < 15.0 mg/L). In the current study, average transparency at Site T1, and DO and ORP across all three sites, fell within the mild black-odor parameters (10–25 cm, 0.2–2.0 mg/L and −200–50 mV, respectively). However, NH_3-N concentrations exceeded 15 mg/L, indicative of severe black-odor conditions [28]. Average TN and TP concentrations were 16.75 mg/L and 1.38 mg/L, respectively, with an N:P ratio of 12.1, suggesting N and P co-limitation in the river's nutrients [29]. NH_3-N constituted 88.9% of the TN, likely due to external pollution imported. Elevated average COD (24 mg/L) and BOD_5 (8.87 mg/L) levels pointed to intensive organic pollutions [30]. The presence of black FeS or metal sulfides, often a primary cause of black odor in polluted waters, was evidenced by Fe^{2+} concentrations ranging from 0.29 to 0.38 mg/L in the Tangmenbang River [6,31]. Additionally, volatile organic sulfur compounds (VOSCs) analysis suggested DMTS as the predominant odor-causing compound, with concentrations ranging from 2081 to 3419 ng/L.

Table 1. Physicochemical properties of water and sediment in Tangmenbang River.

Water		Sediment	
Parameters (Units)	**Mean (Range)**	**Parameters (Units)**	**Mean (Range)**
pH	7.57 (7.57–7.58)	TOC (g/kg)	6.90 (6.80–7.00)
Transparency (cm)	27.7 (25.0–30.0)	NH_3-N (mg/kg)	61.4 (59.6–62.9)
DO (mg/L)	0.40 (0.34–0.46)	TN (mg/kg)	162 (131–197)
ORP (mV)	27.3 (13.8–36.1)	NO_x-N (mg/kg)	3.01 (2.57–3.40)
TN (mg/L)	16.7 (16.2–17.1)	TP (mg/kg)	582 (528–628)
NH_3-N (mg/L)	15.0 (14.6–15.2)	Fe (g/kg)	20.9 (19.6–23.0)
Nitrate (mg/L)	0.21 (0.10–0.41)	Fe/Al-P (mg/kg)	186 (168–196)
TP (mg/L)	1.38 (1.32–1.45)		
COD (mg/L)	24.0 (19.0–28.0)		
BOD_5 (mg/L)	8.87 (8.00–9.70)		
SO_4^{2-} (mg/L)	35.8 (33.6–38.1)		
S^{2-} (mg/L)	0.02 (0.02–0.03)		
Fe^{2+} (mg/L)	0.34 (0.29–0.38)		
Mn^{2+} (mg/L)	0.06 (0.06–0.07)		
DMTS (ng/L)	2824 (2081–3419)		

Surface sediment TOC content ranged from 6.80 to 7.00 g/kg (Table 1), with the C/N ratio exceeding 20, indicating an allochthonous origin for the organic matter [32]. NH_3-N and NO_3-N comprised 38.3% and 1.97% of TN, respectively, pointing to potential nitrification inhibition [33]. A high Fe concentration (19.6–23.0 g/kg) was noted, likely due to extensive metal processing manufacturers around the river, which may significantly affect phosphorus mobility [34]. The ratio of Fe/Al-bond phosphorus (Fe/Al-P) to TP was about 30%, attributed to the low ORP facilitating the reduction of Fe (III) to Fe (II) [35]. Thus, some PO_4^{3-} associated with iron oxides and hydro-oxides, such as hydroferritite and ferritite, could be released into the pore water, resulting in internal pollution [35].

3.2. Performance of Water and Sediment after MNBs Aeration

Figure 3 shows that after 7 days of aeration (corresponding to the first sampling after aeration), the DO, OPR, NH_3-N and transparency measurements significantly surpassed the mild black-odor standards, indicating a rapid improvement in water quality. The process of aeration progressively led to water oxygenation and an aerobic state. The average DO content increased by 89.4% for MNBs aeration and 33.3% for blast aeration, suggesting MNBs's effectiveness in enhancing dissolved oxygen levels [4]. This outcome can be attributed to the MNBs providing a higher surface area for O_2 mass transfer and a higher O_2 vapor pressure to drive the partition balance [14]. The rise in DO was accompanied by an increase in ORP, indicating the prevalence of an oxidizing environment. ORP increased by 75.4% for MNBs treatment and 48.2% for blast aeration. However, a massive sewage influx in October led to a notable decrease in ORP for control and blast aeration treatments, while MNBs maintained stable OPR levels. In this oxidizing environment, the enhanced activities of nitrifying bacteria accelerated the conversion of NH_3-N into NO_3^- or NO_2^-, resulting in a reduction in NH_3-N concentration [9]. The removal efficiency for MNBs remained at 63.2%, which was 25% greater than blast aeration. A temporary elevation of NH_3-N in summer was owing to the abundant rainfalls that carried plenty of pollutants into the river. Furthermore, water transparency improved by 5.5 cm for blast aeration and 22 cm for MNBs. The increase in DO contributed to the degradation of colored dissolved organic matter (cDOM), sulfides and blackening metallic compounds, thereby enhancing water clarity [36]. The superior performance of MNBs was attributed to their higher oxygenation capability [10].

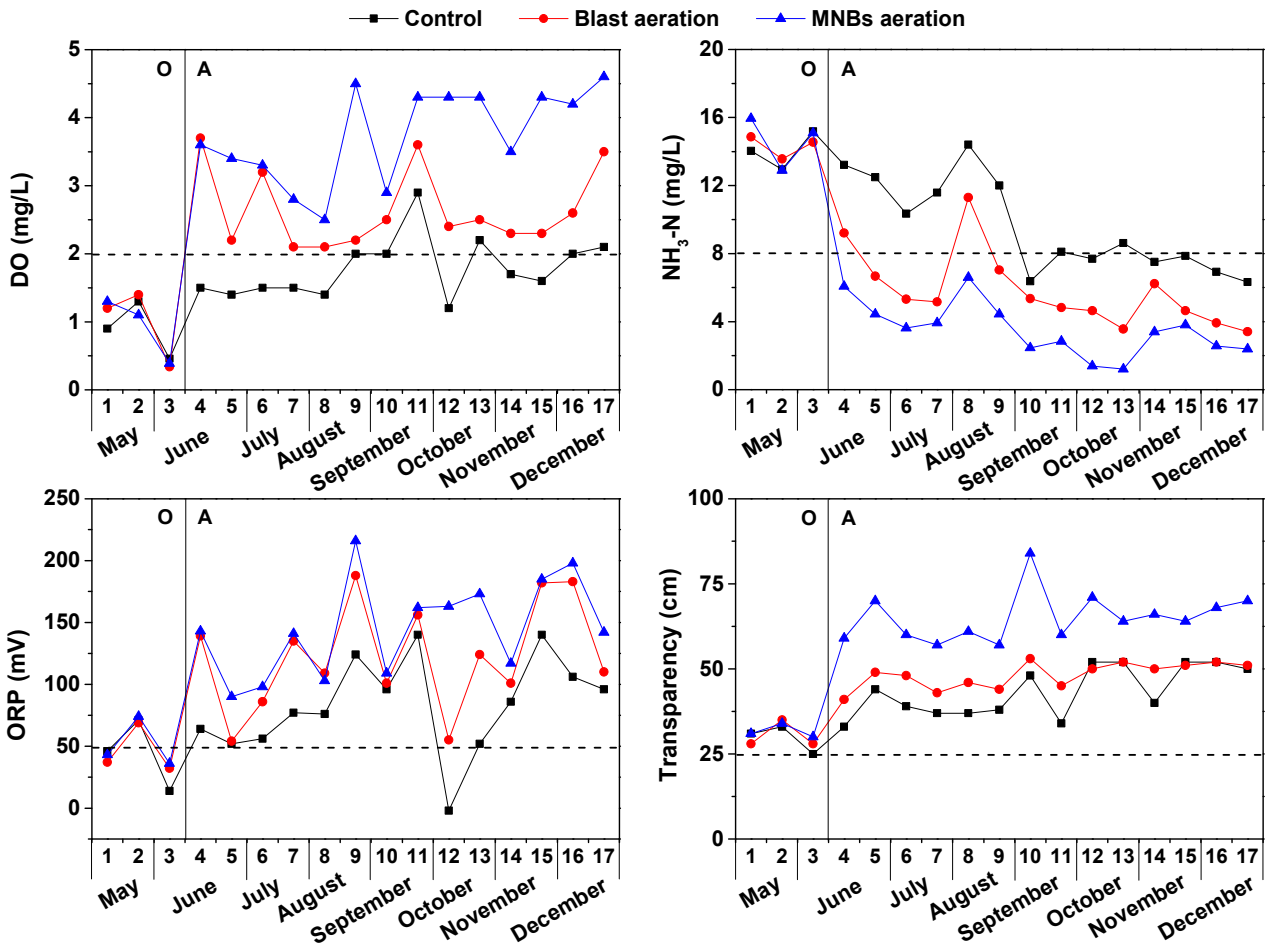

Figure 3. Temporal variation in DO, NH_3-N, OPR and transparency in water under different aerations (the dash lines correspond to the light black-odor degree according to the work guide of urban black and odorous water body remediation from China; the letters "O" and "A" represent the original state and the aeration state, respectively).

At the same time, BOD_5, COD, TN and TP in water samples showed improvement (Figure 4). MNBs aeration demonstrated significantly higher removal efficiencies for BOD_5 (54.4%) and COD (39.0%) compared to traditional pumping systems (31.9% and 16.9%, respectively). The ratio of BOD_5 to COD decreased from 0.37 to 0.20 in the case of MNBs and to 0.24 for blast aeration, indicating substantial degradation of organic matter. This degradation could result from biodegradation by the activated microbial communities or from the direct reaction with reactive oxygen species provided by MNBs collapse [10,37]. Alkaline aeration converted NH_3-N to NH_3, aiding in the elimination of TN [38], with an observed efficiency of about 20% in this study. The MNBs-aerated system achieved a notable TP removal rate of approximately 28%, in contrast to the negligible reduction observed with blast aeration. This difference might stem from the absorption of inorganic macromolecular colloid degraded from organic compounds and metabolism of aerobic bacteria, which expedited the migration of soluble phosphate from the upper water to the sediment [9]. Higher TP concentrations (570 mg/L) in sediment after MNBs aeration compared to other treatments (520 mg/L) support this finding. Furthermore, nearly all the major odor-causing substance, DMTS, was removed within a month or less.

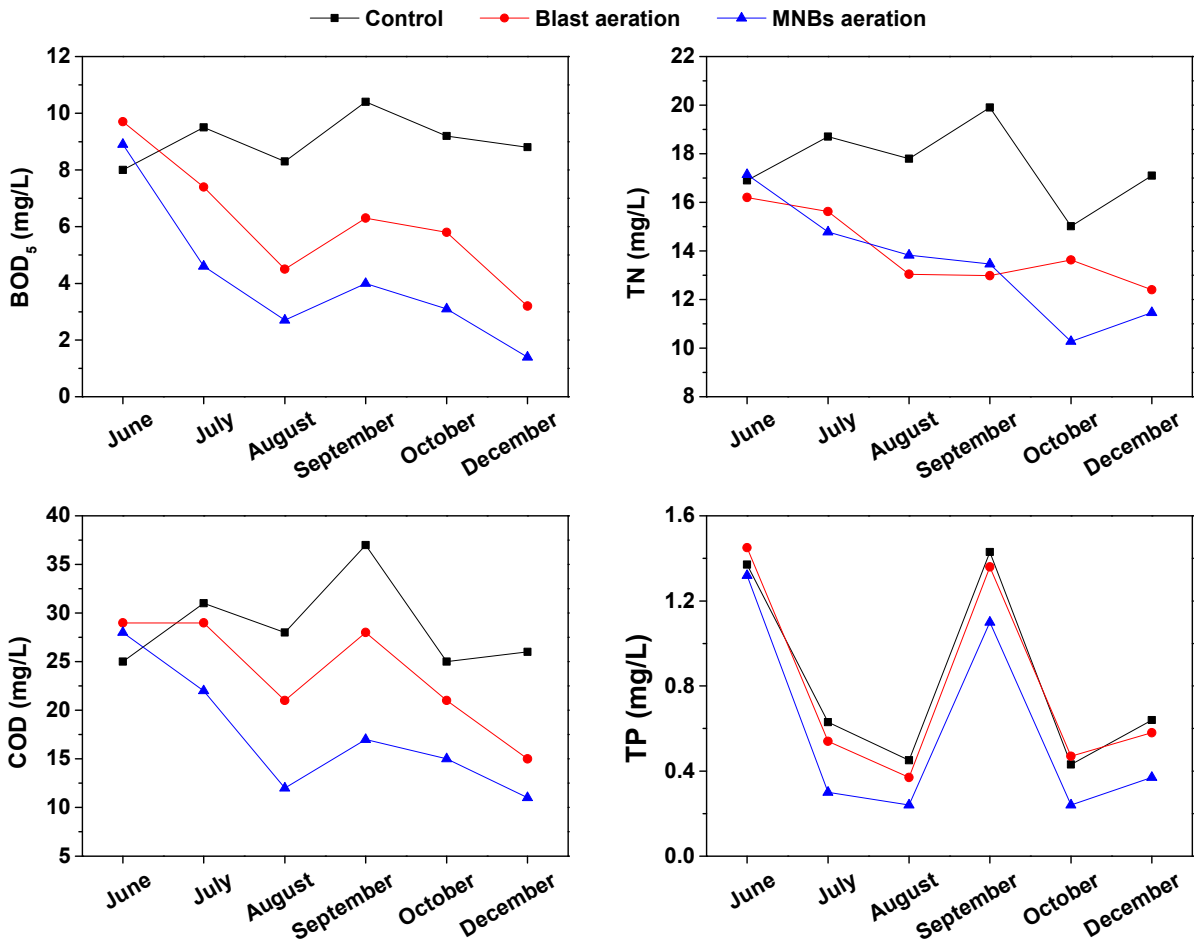

Figure 4. Temporal variation in COD, BOD_5, TN and TP in water under different aerations.

Improved oxygen supply and retention capabilities have effectively inhibited the endogenous release of pollutants from sediments. Specifically, the removal rates of TOC (30.6%) and NH_3-N (39.2%) in sediments treated with MNBs were apparently greater than those in the blast-aerated sediments (10.2% and 7.10%, respectively) (Figure 5). The decomposition and transformation of organic matter in sediments primarily involve humification and mineralization. Enhanced activity of aerobic indigenous microorganisms in the sediment decomposes organic compounds into simpler forms, which then undergo complex polymerization reactions to form humus [39]. Additionally, the mineralization process in Fe-rich sediments likely involves reactions of organic matter with hydroxide or oxide of trivalent iron to produce carbon dioxide [40]. The proliferation of nitrifying bacteria also contributes to increased NH_3-N removal through nitrification. Post-MNBs treatment, the proportion of Fe/Al-P to TP increased from approximately 30% to 55%, speculating that MNBs improve the binding capacity (e.g., adsorption or co-precipitation) of iron(oxy)hydroxides and aluminum hydroxides to phosphorus, thereby inhibiting endogenous phosphorus release from the sediments [34]. The redox potential in oxic and alkaline environments favors higher concentrations of Fe/Al-P [34].

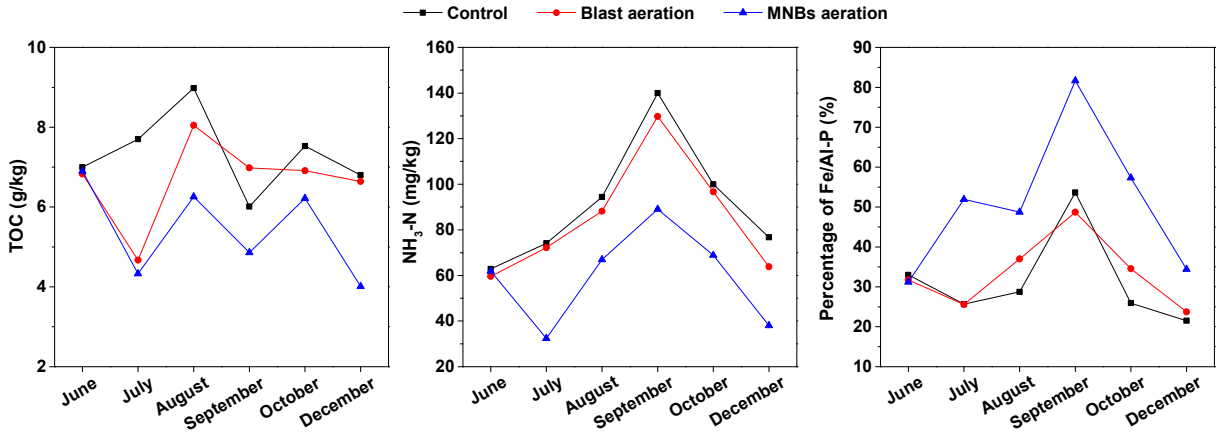

Figure 5. Temporal variation in TOC, NH_3-N and Fe/Al-P in sediment under different aerations.

Statistically significant differences in DO, OPR, NH_3-N, transparency, COD, BOD_5, TN and TOC were observed between the MNBs and control groups (Kruskal–Wallis test, $p < 0.05$). In contrast, only DO, NH_3-N and TN concentrations differed significantly between blast aeration and control groups (Kruskal–Wallis test, $p < 0.05$). MNBs aeration demonstrated superior performance overall. The findings align with prior research indicating that MNBs had a higher oxygen mass transfer coefficient and oxygenation capability for the more effective removal of pollutants [4,9,10]. In this experiment, the average energy consumption was approximately 24 kWh/d in the blast aeration and 28 kWh/d in the MNBs aeration. Although MNBs aeration consumed more energy than blast aeration at the same working time, it achieved higher oxygen transfer efficiency (Figure 2b). When considering the daily average energy consumption per gram of pollutant removed, the energy efficiency ratios of MNBs to blast aeration for NH_3-N, BOD_5, COD, TN and TP in water samples were 0.72, 0.68, 0.50, 1.03 and 0.15, respectively. MNBs and blast aeration showed similar energy consumption for the TN removal. However, MNBs exhibited better potential and economy for NH_3-N, BOD_5, COD and TP removal than macro bubbles.

3.3. Response of Plankton Composition in Water to MNBs Aeration

The phytoplankton community identified in water samples included *Cyanophyta*, *Chlorophyta*, *Bacillariophyta*, *Euglenophyta*, *Cryptophyta*, *Pyrrophyta* and *Cryptophyta*, in which the abundance of *Cyanophyta*, *Chlorophyta* and *Bacillariophyta* had absolute superiority. The dominant species of *Cyanophyta* were *Planktothrix* and *Limnothrix*, and the *Chlorophyta* were dominated by *Chlamydomonas*. Normally, the disintegration of algae was accompanied by the production of bad taste and odor, and some species even generated a toxic secondary metabolite (e.g., cyanotoxins) that was harmful to animals and humans [1]. The zooplankton community identified in the current study included *protozoa*, *rotifers*, *copepods* and *cladocerans*, and it was dominated by *protozoa* and *rotifers*. The *protozoa* were dominated by *Tintinnopsis kiangsuensis*, *Vorticella* sp. and *Leprotintinnus fluviatile*, with biomasses of 0.75–3.00 mg/L, 0.00–2.8 mg/L and 0.06–2.76 mg/L, respectively. The *rotifers* were dominated by *Brachionus calyciflorus* with a biomass of 0.06–1.63 mg/L.

Monthly variations in the species and biomass of plankton were observed in Figures 6 and 7. Notably, a surge in zooplankton boom corresponded with a substantial decline in phytoplankton biomass throughout the monitoring process (Figure 6). For instance, in July, zooplankton reached their peak biomass (6.64–16.0 mg/L), while phytoplankton biomass was at its lowest (0.45–1.15 mg/L). This trend likely resulted from zooplankton predation on algae. Overall, post-MNBs aeration, plankton biomass was lower compared to other treatments, suggesting MNBs's inhibitory effect on plankton. This reduction can be attributed to two factors: firstly, aeration-induced depletion of nitrogen and phosphorus in water, limiting plankton growth; and secondly, potential disruption of plankton cell structures by MNBs, leading to their rapid settling [41]. On the contrary, a low S-W diversity

index was recorded (Figure 7), ranging from 0.24 to 1.25 for phytoplankton and 0.00 to 0.70 for zooplankton. This indicates a relatively simple community structure of plankton, with minimal inter-species competition contributing to increased community instability [42].

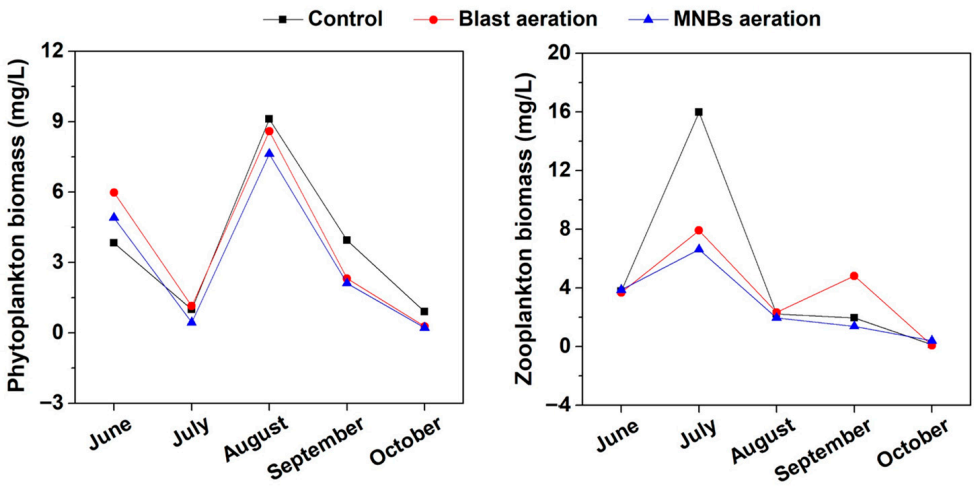

Figure 6. Temporal variation in phytoplankton biomass and zooplankton biomass in different aerations.

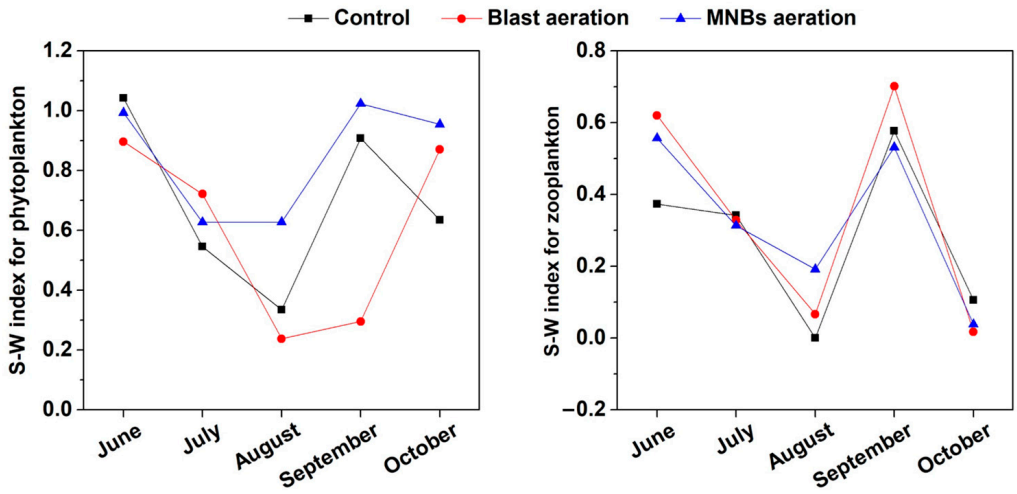

Figure 7. Shannon–Wiener index for phytoplankton and zooplankton in different aerations.

3.4. Impacts of MNBs on Microbial Community in Sediment

Figure 8 illustrates the relative abundance of microorganisms at the phylum level in various sediment samples. The dominant microbial phylum in original sediment included *Chloroflexi*, *Proteobacteria*, *Acidobacteriota*, *Actinobacteria*, *Firmicutes*, *Desulfobacterota* and *Bacteroidota*, accounting for about 80% of the total sequences (Figure 8a). Notably, *Chloroflexi* and *Proteobacteria* were the most abundant, which was in accordance with other studies [1,43–45]. *Chloroflexi*, a photoautotrophic bacterium, typically thrives in nutritionally adequate environments [43], implying a high nutrient level in the sediment. Both *Chloroflexi* and *Proteobacteria* are known for their ability to decompose organic compounds [46,47]. Additionally, certain species of *Proteobacteria* are functional microbial groups involved in nitrogen and sulfur metabolism [48]. After restoration (5 months), the bacterial community structures in sediments from the control and blast aeration sites showed similarity (Figure 8b,c), suggesting a minimal impact of blast aeration on the microbial community. Conversely, the sediment subjected to MNBs aeration exhibited a significant alteration in bacterial community structure (Figure 8d). The relative abundance of *Actinobacteria*, *Firmicutes* and *Myxococcota* remarkably increased, and accordingly, *Chloroflexi* and *Proteobacteria* were significantly reduced (Fisher's exact test, $p < 0.001$). MNBs aeration demonstrated

a stronger selectivity for microorganisms, effectively inhibiting the growth of anaerobic species in water and promoting aerobic species as the dominant strains [17]. These findings corroborate the marked increase in aerobic microorganisms post-MNBs aeration, enhancing the self-purification capacity of the water.

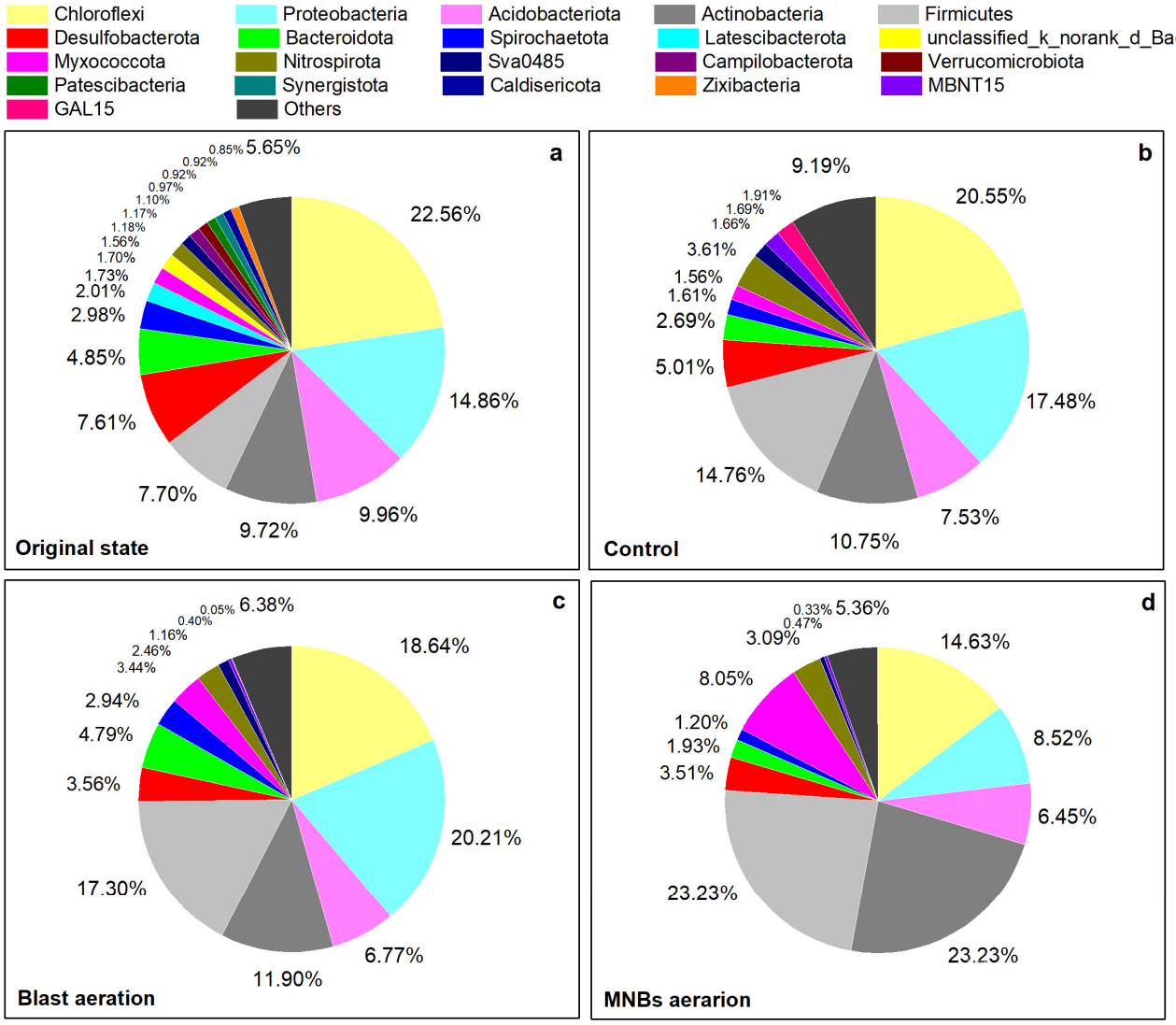

Figure 8. Composition of microbial community at the phylum level for the sediment from original state (**a**), control (**b**), blast aeration (**c**) and MNBs aeration (**d**) (the relative abundance of less than 0.01% are uniformly indicated by others).

At the class level, Gammaproteobacteriam, Anaerolineae, Clostridia, Actinobacteria, Bacilli and Alphaproteobacteria were identified as the dominant bacteria in sediment from both control and blast aeration, whereas sediments treated with MNBs predominantly harbored Gammaproteobacteriam, Anaerolineae, Clostridia, Actinobacteria, Myxococcia and Bacteroidia (Figure 9a). Fisher's exact test revealed significant differences in a total of 15 microorganisms between the control and MNBs aeration treatments ($p < 0.006$, Figure 9b). Post-MNBs aeration, the relative abundance of Clostridia, Actinobacteria and Myxococcia increased by over 5%, while Acidimicrobiia, Desulfitobacteriia and Ktedonobacteria showed a rise of more than 2%. Particularly, Acidimicrobiia, an oligotrophic bacteria, includes chemoautotrophs capable of oxidizing Fe (II) to Fe (III) using CO_2 as a carbon source [49,50]. Desulfobacterota mediates sulfide oxygenation, and the rate is 1000 to 10,000 times faster than the abiotic oxidation rate [48]. Concurrently, the relative abundance of Anaerolineae, Gammaproteobacteria, Bacilli and Alphaproteobacteria decreased by

over 2%, with Anaerolineae experiencing a maximum reduction of approximately 10%. These results interpret that MNBs aeration can effectively inhibit the growth of anaerobic microorganisms and reduce their abundance in sediment [51].

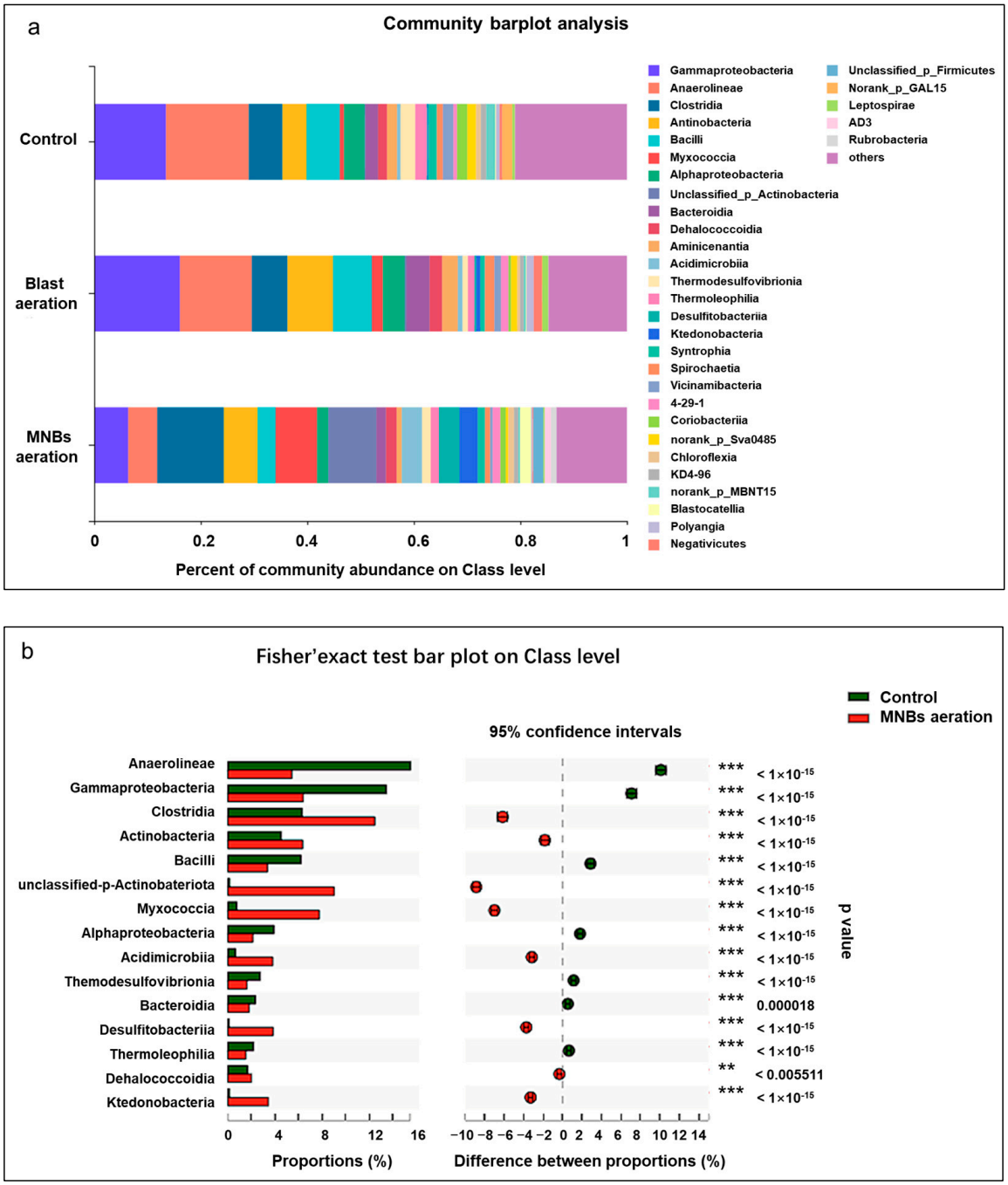

Figure 9. (**a**) Relative abundances of microbial community structures in sediment from different treatments at the class level. (**b**) The difference in microbial composition and relative abundance of sediment from treatment of control and MNBs aeration at class level (* represented significance: **, $p < 0.01$; ***, $p < 0.001$).

4. Conclusions

Compared to conventional aeration, MNBs enhance oxygen transfer and facilitates the removal of organics, nutrients, VOSCs, blacking substances and plankton, thereby rapidly improving water quality. Simultaneously, MNBs promote the transformation of soluble phosphorus into Fe/Al-P in sediment, inhibiting the release of endogenous phosphorus.

Furthermore, MNBs augment the activities of aerobic microorganisms, establishing them as dominant strains and enhancing the self-purification capacity of water. Thus, MNBs present a great potential for treating black-odorous water bodies.

Supplementary Materials: The following supporting information can be downloaded at: https://www.mdpi.com/article/10.3390/su152416695/s1, Figure S1: Distribution of 7 sewage discharge outlets; Figure S2: (**a**) An egg-shaped bubble generator, (**b**) Micro MNBs aeration generator.

Author Contributions: Conceptualization, Q.X. and Z.Z.; methodology, Q.X. and Z.Z.; software, Q.X. and Z.Z.; validation, Q.X., Z.Z. and X.C.; formal analysis, Q.X. and Z.Z.; investigation, Q.X., Z.Z. and X.C.; resources, X.C.; data curation, Z.Z.; writing—original draft preparation, Q.X.; writing—review and editing, Z.Z. and X.C.; visualization, Q.X. and Z.Z.; supervision, X.C.; project administration, X.C.; funding acquisition, X.C. All authors have read and agreed to the published version of the manuscript.

Funding: This research received no external funding.

Institutional Review Board Statement: Not applicable.

Informed Consent Statement: Not applicable.

Data Availability Statement: The data presented in this study are available in the article.

Acknowledgments: We would like to express our sincere gratitude to the State Key Laboratory of Pollution Control and Resource Reuse for providing equipment and advice during this study.

Conflicts of Interest: The authors declare no conflict of interest.

References

1. Liu, Q.; Wu, H.; Huang, C.; Lin, H.; Li, W. Microbial compositions, ecological networks, and metabolomics in sediments of black-odour water in Dongguan, China. *Environ. Res.* **2022**, *210*, 112918. [CrossRef] [PubMed]
2. Chen, C.; Yang, X.; Luo, H.; Zeng, D.; Huang, S. Linking microbial community and biological functions to redox potential during black-odor river sediment remediation. *Environ. Sci. Pollut. Res.* **2020**, *27*, 40392–40404. [CrossRef] [PubMed]
3. Wang, F.; Wang, H.; Zhao, Z.; Dong, W.; Wu, Z.; Zhang, S.; Li, W.; Wu, X. Simultaneous elimination of black-odor and stabilization of heavy metals in contaminated sediment using calcium peroxide/hydroxyapatite: Microbial responses and ecotoxicological effects. *J. Hazard. Mater.* **2022**, *429*, 128298. [CrossRef] [PubMed]
4. Chen, B.; Zhou, S.; Zhang, N.; Liang, H.; Sun, L.; Zhao, X.; Guo, J.; Lu, H. Micro and nano bubbles promoted biofilm formation with strengthen of COD and TN removal synchronously in a blackened and odorous water. *Sci. Total Environ.* **2022**, *837*, 155578. [CrossRef] [PubMed]
5. Zhang, D.; Yang, H.; Lan, S.; Wang, C.; Xie, Y. Evolution of urban black and odorous water: The characteristics of microbial community and driving-factors. *J. Environ. Sci.* **2022**, *112*, 94–105. [CrossRef] [PubMed]
6. Li, P.; Ye, J.; Zhang, W.; Hu, F.; Guo, Q.; Xu, Z. The blackening process of black-odor water: Substance types determination and crucial roles analysis. *J. Hazard. Mater.* **2023**, *443*, 130295. [CrossRef] [PubMed]
7. Huang, Y.H.; Liu, Y.; Du, P.P.; Zeng, L.J.; Mo, C.H.; Li, Y.W.; Lu, H.; Cai, Q.Y. Occurrence and distribution of antibiotics and antibiotic resistant genes in water and sediments of urban rivers with black-odor water in Guangzhou, South China. *Sci. Total Environ.* **2019**, *670*, 170–180. [CrossRef]
8. Ministry of Ecology and Environment. *Action Plan for Water Pollution Prevention and Control*; Ministry of Ecology and Environment: Beijing, China, 2015. Available online: https://www.mee.gov.cn/zcwj/gwywj/201811/t20181129_676575.shtml (accessed on 15 September 2023).
9. Liu, M.; Li, T.; Wang, Z.; Radu, T.; Jiang, H.; Wang, L. Effect of aeration on water quality and sediment humus in rural black-odorous water. *J. Environ. Manag.* **2022**, *320*, 115867. [CrossRef]
10. Lyu, T.; Wu, Y.; Zhang, Y.; Fan, W.; Wu, S.; Mortimer, J.G.R.; Pan, G. Nanobubble aeration enhanced wastewater treatment and bioenergy generation in constructed wetlands coupled with microbial fuel cells. *Sci. Total Environ.* **2023**, *895*, 165131. [CrossRef]
11. Zhou, S.; Nazari, S.; Hassanzadeh, A.; Bu, X.; Ni, C.; Peng, Y.; Xie, G.; He, Y. The effect of preparation time and aeration rate on the properties of bulk micro-nanobubble water using hydrodynamic cavitation. *Ultrason. Sonochem.* **2022**, *84*, 105965. [CrossRef]
12. Soyluoglu, M.; Kim, D.; Zaker, Y.; Karanfil, T. Stability of Oxygen Nanobubbles under Freshwater Conditions. *Water Res.* **2021**, *206*, 117749. [CrossRef] [PubMed]
13. Lyu, T.; Wu, S.; Mortimer, J.G.R.; Pan, G. Nanobubble technology in environmental engineering: Revolutionization potential and challenges. *Environ. Sci. Technol.* **2019**, *53*, 7175–7176. [CrossRef] [PubMed]
14. Xue, S.; Zhang, Y.; Marhaba, T.; Zhang, W. Aeration and dissolution behavior of oxygen nanobubbles in water. *J. Colloid Interface Sci.* **2022**, *609*, 584–591. [CrossRef] [PubMed]
15. Wu, Y.; Tian, W.; Zhang, Y.; Fan, W.; Liu, F.; Zhao, J.; Wang, M.; Liu, Y.; Lyu, T. Nanobubble technology enhanced ozonation process for ammonia removal. *Water* **2022**, *14*, 1865. [CrossRef]

16. Tang, Y.; Zhang, M.; Zhang, J.; Lyu, T.; Cooper, M.; Pan, G. Reducing arsenic toxicity using the interfacial oxygen nanobubble technology for sediment remediation. *Water Res.* **2021**, *205*, 117657. [CrossRef] [PubMed]
17. Wang, S.; Liu, Y.; Li, P. Effect of micro-nano bubble aeration on aerobic microbial community in small water body. *China Water Wastewater* **2020**, *36*, 29–34.
18. Zhou, Z.; Chai, X. Research on the rapid removal of odorous compounds in black and odorous water by micro-nano aeration. *Shandong Chem. Ind.* **2021**, *2*, 253–257.
19. Ma, J.; Lin, X.; Yu, Z.; Wang, X.; Chen, J.; He, Q. Characterization, risk assessment and resource potential of sediments in the black-odor water in Hunan, China. *Environ. Monit. Assess.* **2022**, *194*, 1–11. [CrossRef]
20. Lu, P.; Lin, Y.H.; Yang, Z.Q.; Xu, Y.P.; Tan, F. Effects of application of corn straw on soil microbial community structure during the maize growing season. *J. Basic Microbiol.* **2014**, *54*, 1–11. [CrossRef]
21. Wang, D.; Nie, L.; Li, J. Transfer characteristics of nutrient elements through hydrological process of Pinus tabulaeformis stad in Beijing Xishan area. *Acta Ecol. Sin.* **2006**, *26*, 2101–2107.
22. Song, Q.; Li, Y.; Jiang, X. Spatial distribution of phosphorus fractions in the sediments of Meiliang Bay, Taihu Lake, China. *Adv. Mater. Res.* **2012**, *610–613*, 2766–2770. [CrossRef]
23. Herath, I.K.; Wu, S.; Ma, M.; Ping, H. Heavy metal toxicity, ecological risk assessment, and pollution sources in a hydropower reservoir. *Environ. Sci. Pollut. Res.* **2022**, *29*, 32929–32946. [CrossRef] [PubMed]
24. Ma, X.; Feng, J.; Song, Y.; Ni, M.; Dietrich, A.M.; Chen, C.; Li, Q.; Gao, N. Release behavior of odor contaminants derived from Microcystis aeruginosa in rivers and a non-strict anaerobic aqueous system. *AQUA* **2015**, *64*, 812–823.
25. Weng, B.; Yang, Y.; Yan, D.; Wang, J.; Dorjsuren, B. Shift in plankton diversity and structure: Influence of runoff composition in the Nagqu River on the Qinghai-Tibet Plateau. *Ecol. Indic.* **2020**, *109*, 105818. [CrossRef]
26. Walters, W.; Hyde, E.R.; Berg-Lyons, D.; Ackermann, G.; Humphrey, G.; Parada, A.; Gilbert, J.A.; Jansson, J.K.; Caporaso, J.G.; Fuhrman, J.A. Improved Bacterial 16S rRNA Gene (V4 and V4-5) and Fungal Internal Transcribed Spacer Marker Gene Primers for Microbial Community Surveys. *Msystems* **2016**, *1*, 9–15. [CrossRef] [PubMed]
27. Yang, B.; Jiang, Y.J.; He, W.; Liu, W.X.; Kong, X.Z.; Jørgensen, S.E.; Xu, F.L. The tempo-spatial variations of phytoplankton diversities and their correlation with trophic state levels in a large eutrophic Chinese lake. *Ecol. Indic.* **2016**, *66*, 153–162. [CrossRef]
28. Ministry of Housing and Urban Rual Development. *The Work Guide of Urban Black and Odorous Water Body Remediation*; Ministry of Housing and Urban Rual Development: Beijing, China, 2015; pp. 1–34.
29. Qin, B.; Zhou, J.; Elser, J.J.; Gardner, W.S.; Deng, J.; Brookes, J.D. Water Depth Underpins the Relative Roles and Fates of Nitrogen and Phosphorus in Lakes. *Environ. Sci. Technol.* **2020**, *54*, 3191–3198. [CrossRef] [PubMed]
30. Dkmen, F. Temporal Variation of Biological Oxygen Demand (BOD), Chemical Oxygen Demand (COD), and pH Values in Surface Waters of Gölcük-Kocaeli, Turkey. In *Plants, Pollutants and Remediation*; Öztürk, M., Ashraf, M., Aksoy, A., Ahmad, M.S.A., Hakeem, K.R., Eds.; Springer: Dordrecht, The Netherlands, 2015; pp. 341–347.
31. Duval, B.; Ludlam, D.S. The Black Water Chemocline of Meromictic Lower Mystic Lake, Massachusetts, USA. *Int. Rev. Hydrobiol.* **2001**, *86*, 165–181. [CrossRef]
32. Dong, S.; Li, Z.; Chen, Q.; Zhiqiao, W. Total organic carbon and its environmental significance for the surface sediments in groundwater recharged lakes from the Badain Jaran Desert, Northwest China. *J. Limnol.* **2018**, *77*, 121–129. [CrossRef]
33. Stockenberg, A.; Johnstone, R.W. Benthic Denitrification in the Gulf of Bothnia. *Estuar. Coast. Shelf Sci.* **1997**, *45*, 835–843. [CrossRef]
34. León, J.G.; Pedrozo, F.L.; Temporetti, P.F. Phosphorus fractions and sorption dynamics in the sediments of two Ca-SO4 water reservoirs in the central Argentine Andes. *Int. J. Sediment Res.* **2017**, *32*, 442–451. [CrossRef]
35. Kim, L.H.; Choi, E.; Stenstrom, M.K. Sediment characteristics, phosphorus types and phosphorus release rates between river and lake sediments. *Chemosphere* **2003**, *50*, 53–61. [CrossRef] [PubMed]
36. Xiao, Y.; Wang, Y.; Wu, Y.; Zeng, C.; Zheng, W. Applicationof black-odorriverof aerobic-oxygen-enrichedaerationbiological treatment in-situremediation. *Chin. J. Environ. Eng.* **2017**, *11*, 2780–2784.
37. Zhou, S.; Liu, M.; Chen, B.; Sun, L.; Lu, H. Microbubble- and nanobubble-aeration for upgrading conventional activated sludge process: A review. *Bioresour. Technol.* **2022**, *362*, 127826. [CrossRef] [PubMed]
38. Gin, Y.H.; Gopalakrishnan, A.P. Sediment Oxygen Demand and Nutrient Fluxes for a Tropical Reservoir in Singapore. *J. Environ. Eng.* **2010**, *136*, 78–85. [CrossRef]
39. Goñi, M.A.; Thomas, K.A. Sources and transformations of organic matter in surface soils and sediments from a tidal estuary (North Inlet, South Carolina, USA). *Estuaries* **2000**, *23*, 548–564. [CrossRef]
40. Roden, E.E.; Wetzel, R.G. Competition between Fe(III)-reducing and methanogenic bacteria for acetate in iron-rich freshwater sediments. *Microb. Ecol.* **2003**, *45*, 252–258. [CrossRef]
41. Li, P.; Song, Y.; Yu, S. Removal of Microcystis aeruginosa using hydrodynamic cavitation: Performance and mechanisms. *Water Res.* **2014**, *62*, 241–248. [CrossRef]
42. Xu, C.; Yang, J.; Ma, M.; Hu, X.; You, W. Characteristics of Phytoplankton Community Changes in Dianshan Lake During Peak Period of Algal Blooms. *Environ. Sci.* **2012**, *33*, 1136–1145.
43. Zhao, L.; Liu, Y.; Wang, Y.; Zhao, R.; Ren, W.; Xu, M. Bacterial community structure and diversity of sediments in a typical plateau lakeshore. *Microbiol. China* **2020**, *47*, 401–410.

44. Shen, X.; Xu, M.; Li, M.; Zhao, Y.; Shao, X. Response of sediment bacterial communities to the drainage of wastewater from aquaculture ponds in different seasons. *Sci. Total Environ.* **2020**, *717*, 137180. [CrossRef] [PubMed]
45. Shao, Y.; He, Q.; Fu, Y.; Liu, Y. Construction of the comprehensive evaluation system of waterbody pollution degree and the response of sedimentary microbial community. *Environ. Pollut.* **2023**, *317*, 120837. [CrossRef] [PubMed]
46. Yi, M.; Zhang, L.; Qin, C.; Lu, P.; Yuan, S. Temporal changes of microbial community structure and nitrogen cycling processes during the aerobic degradation of phenanthrene. *Chemosphere* **2021**, *1*, 131709. [CrossRef] [PubMed]
47. Chang, W.; Sun, J.; Pang, Y.; Zhang, S.; Xu, R. Effects of different habitats on the bacterial community composition in the water and sediments of Lake Taihu, China. *Environ. Sci. Pollut. Res.* **2020**, *27*, 44983–44994. [CrossRef]
48. Liu, P. Studies on the microorganisms of three domains associated with seagrass (*Zostera japonica*) meadows: Distributions, ecological functions, and environmental drivers. In *Marine Biology 2022*; University of Chinese Academy of Sciences: Yantai, China, 2022; p. 193.
49. Zhang, L.; Zhao, T.; Shen, T.; Gao, G. Seasonal and spatial variation in the sediment bacterial community and diversity of Lake Bosten, China. *J. Basic Microbiol.* **2018**, *59*, 224–233. [CrossRef]
50. He, Y.; Long, L.; Tian, X. Recent advances in the class Acidimicrobiia. *Microbiol. China* **2020**, *47*, 1945–1957.
51. Xu, X. The research of in-situ remediation black-ordorous river by aeration enhancing functional strains. In *Environmental Science and Engineering 2017*; Chengdu University of Technology: Chengdu, China, 2017; p. 60.

Disclaimer/Publisher's Note: The statements, opinions and data contained in all publications are solely those of the individual author(s) and contributor(s) and not of MDPI and/or the editor(s). MDPI and/or the editor(s) disclaim responsibility for any injury to people or property resulting from any ideas, methods, instructions or products referred to in the content.